CEBAF-PR-86-012

SPIN PHYSICS AT INTERMEDIATE ENERGIES

Summary report (Part I) of the Parallel Session 3,
Spin Physics at Intermediate Energies (Theory and Experiment)
INTERNATIONAL SYMPOSIUM ON HIGH ENERGY SPIN PHYSICS
Protvino, USSR, September 22-28, 1986

Volker Burkert
Continuous Electron Beam Accelerator Facility
12070 Jefferson Avenue
Newport News, VA 23606

CONTINUOUS
ELECTRON
BEAM
ACCELERATOR
FACILITY

SURA SOUTHEASTERN UNIVERSITIES RESEARCH ASSOCIATION

CEBAF

Newport News, Virginia

SPIN PHYSICS AT INTERMEDIATE ENERGIES*

V. Burkert

CEBAF
12070 Jefferson Avenue
Newport News, Va. 23606, USA

*Summary report (Part I) of the Parallel Session 3, 'Spin Physics at Intermediate Energies (Theory and Experiment),' International Symposium on High Energy Spin Physics, September 22 - 28, 1986, Protvino, USSR.

In this session a total of 25 contributed papers were presented studying a broad range of spin effects in nucleons and nuclei using electromagnetic (electrons and photons) and hadronic (pions and nucleons) probes. The status of the theory was characterized by its almost total absence. Only one theoretical contribution was presented at this session. Nucleon-nucleon, nucleon-deuteron and pion-nucleon spin physics were well represented in the plenary sessions/22/, and most of the data which were shown in the parallel session were discussed there as well. This may justify our approach of highlighting those experiments examining electromagnetic-, electroweak- and weak-strong interactions which were not represented in the plenary sessions.

I. Parity Violation in Neutral Current Interactions.

Results were presented from experiments which searched for parity violation effects (1) in quasielastic electron scattering off ^{9}Be /1/, (2) in proton-proton total cross section measurements /2/, and (3) in photodisintegration of deuterium near threshold /3/.

I.1 Quasielastic Electron Scattering Off ^{9}Be .

In low energy ($Q^2 << M_{Z^o}{}^2$) neutral current interactions the parity violating contribution arises from the interference between the one-photon exchange and the neutral weak boson (Z^o) exchange graphs (Fig.1). In electron scattering the interaction contains an isoscalar as well as an isovector piece in both, the vector (V_μ) and axial vector (A_μ) coupling. The effective Lagrangian which describes the parity-nonconserving (PNC) part of the interaction for electron-hadron scattering writes[4]

$$L_{eff} = -G_F/\sqrt{2}[\bar{e}\gamma_\mu\gamma_5 e(\alpha V_\mu{}^3+\gamma V_\mu{}^o) + \bar{e}\gamma_\mu e(\beta A_\mu{}^3+\delta A_\mu{}^o)]$$

The α, β, γ, δ denote the respective coupling constants which have to be determined experimentally. In the Glashow-Salam-Weinberg Model (GSW) of electroweak interaction these coupling constants can be expressed in terms of a single parameter, the electroweak mixing angle θ_W. By choosing appropriate kinematical conditions for electron scattering from nucleons and nuclear targets, one can determine the couplings by a set of four linearly independent measurements.

The SLAC $D(\vec{e},e')X$ scattering experiment[5], in conjunction with atomic physics[6] experiments enabled a model independent measurement of α, γ. The reported Mainz experiment measures a different combination of α, β, γ, δ and allows the extraction of a combination of β and δ, using the previously obtained results as an input. In order to fully appreciate the experimental effort by the Mainz group one should remember that the SLAC experiment had to measure an asymmetry of 10^{-4} at $Q^2 = 1\ (\mathrm{GeV}/c)^2$, whereas the Mainz experiment was performed at $Q^2 = 0.15\ (\mathrm{GeV}/c)^2$ with an expected asymmetry $< 10^{-5}$.

The experimental setup is shown in Fig.2. The polarized electron beam is generated in a GaAs photocathode, illuminated by a circularly polarized

Fig. 1 Diagrams contributing to the dominant PNC effect at low and intermediate energies.

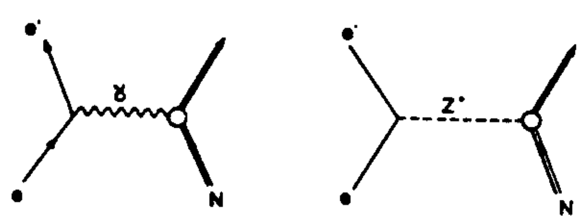

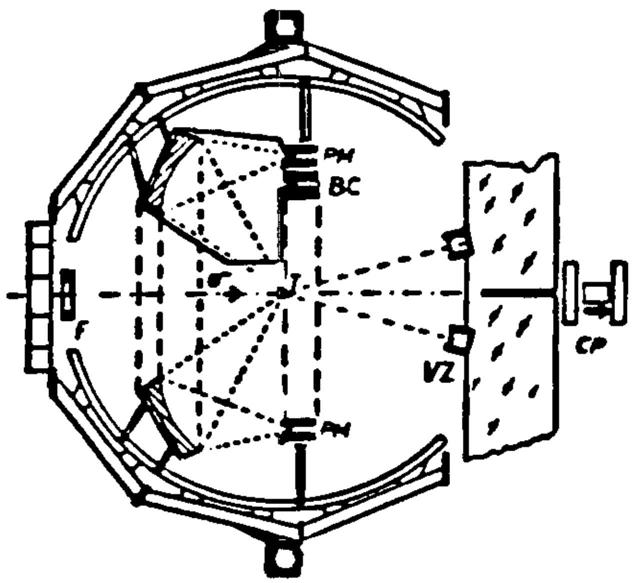

Fig. 2 Arrangement of the Mainz experiment. The scattered electrons are detected in Cerenkov counter setup, covering a solid angle of 2.5 sterad.

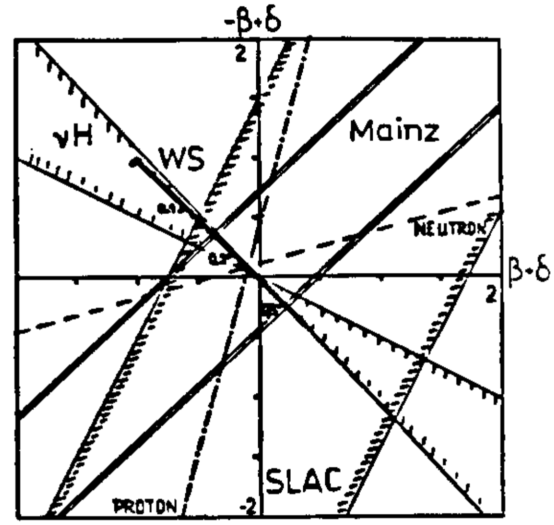

Fig. 3 Area plot of the β, δ coupling constants. The bands labelled 'Mainz', 'SLAC', and 'νH' indicate the areas allowed by the respective experiments at 90% c.l. Also included are the prediction of the GSW model and the lines that would be defined by elastic ep and en scattering.

pulsed laser beam. The electrons are accelerated up to 300 MeV in the linear accelerator. The sign of the polarization (P_e=45%) is reversed statistically between the two pulses by means of a $\lambda/2$ plate positioned in front of the Pockels cell that changes the helicity of the circularly polarized light. The electron beam strikes a ^{9}Be target. Electrons scattered in an angular range $115° < \theta_e < 145°$ are detected in a set of symmetrically arranged gas Cerenkov counters. The kinematics and acceptances are chosen such that quasielastic scattered electrons are detected in the counters with a small contamination of inelastic events only. Because of the large rate required for a sensible measurement, individual events could not be counted. Therefore the Cerenkov counter signal was integrated over the primary beam pulse length. The averaged experimental asymmetry was measured to

$$A_{exp} = -(3.3 \pm 1.1)\times 10^{-8}$$

With a carefully designed monitoring system for the beam position, energy, and current, in the opposite polarization states, spurious asymmetries could be kept $< 3\times10^{-7}$. Using the results of the SLAC measurement and of atomic physics experiments on $\alpha = -0.67 \pm 0.19$ and $\gamma = 0.22 \pm 0.12$, the following relation was obtained:

$$\beta - 0.03\delta = (-0.07 \pm 0.2) .$$

This defines the allowed band in Fig.3. The result agrees with the GSW prediction for the most probable value of $\sin^2\theta_W = 0.226 \pm 0.005$ [7].

It is planned to continue these measurements at the Mainz microtron. Measuring elastic ep and en scattering would give a different sensitivity to the coupling constants. An isolation of the isovector part would be achieved by measuring $\Delta(1232)$ production.

I.2 Parity Violation in Proton-Proton Total Cross Section Measurement.

In pure hadronic interactions the parity violation arises as a result of an interference between amplitudes with a strong coupling at both vertices and amplitudes where one of the vertices is due to the weak neutral coupling (Fig.4).

Parity violation effects have been observed in the decay and in γ emission of nuclei. Uncertainties in the understanding of the nuclear structure, however, render the interpretation difficult. In proton-proton scattering the nuclear structure uncertainties are minimized. Theoretically the low energy measurements are well described by meson contributions. At high energies one may hope to learn about neutral weak interaction effects involving quark-quark scattering (Fig.5).

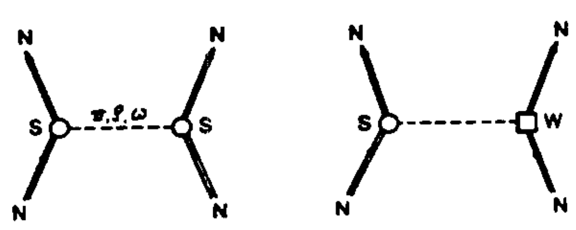

Fig. 4 Diagrams contributing to strangeness conserving neutral weak effects in hadronic reactions. The dominant PNC effects arises from interference between these diagrams.

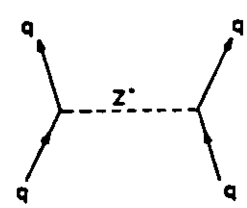

Fig. 5 Contribution to PNC in hadronic reactions at high energies.

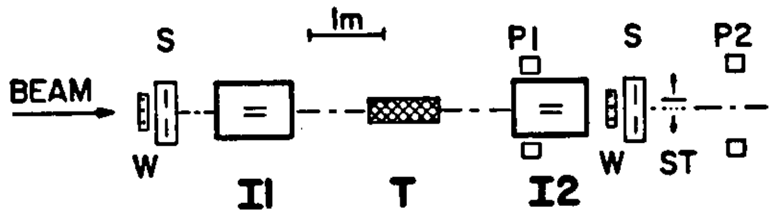

Fig. 6 Schematic arrangement of the LAMPF experiment to measure parity violation effects in the total proton-proton scattering cross section at 800 MeV. The ionization chambers are used to measure the proton transmission through the lH_2 target. The other detectors serve for controlling beam parameters that may create spurious asymmetries.

Results were reported from a LAMPF experiment which measured the total pp scattering cross section asymmetry using an 800 MeV, longitudinally polarized beam, scattered off a 1m long liquid hydrogen target[7]. The total cross section was determined by measuring the transmission through the target with integrating ionization chambers in front of and after the target (Fig.6). The other detectors were used to monitor and control beam parameters that could have created spurious asymmetries for the two polarization directions. In this way the systematic asymmetries could be kept at the level of 10^{-8}. The measured longitudinal asymmetry is

$$A_L = (2.4 \pm 1.1 \pm 0.1)\mathrm{x}10^{-7} .$$

The LAMPF result is shown in Fig.7 together with results of previous measurements performed at 15 MeV[8], 45 MeV[9] and at 6 GeV/c[10], using an H_2O target. Included also are some model calculations. The LAMPF result allows to rule out the wave function renormalization model[11]. In addition, the quark bag prediction[12] fails to reproduce the data at the 2.5σ level. Clearly, it would be very important to go to much higher energies to study weak neutral current quark-quark interactions. This, however, would require a complete understanding of the 'normal' hadronic weak-strong interference effects.

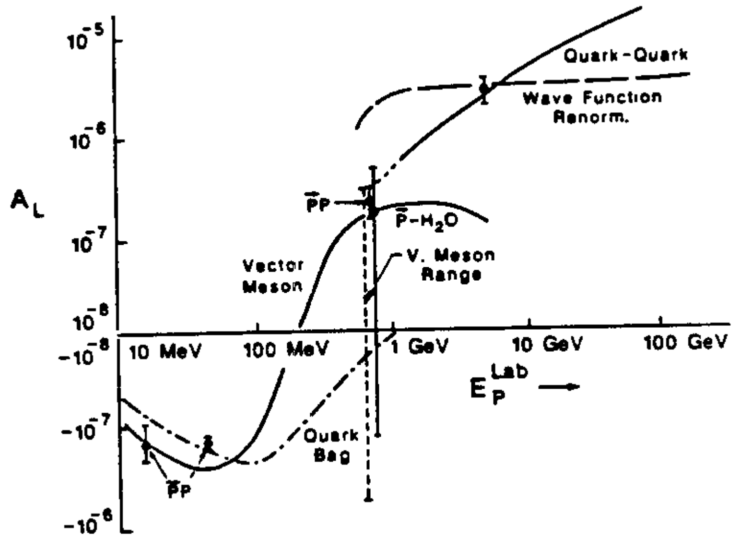

Fig. 7 Parity non-conservation in proton-proton and proton-nucleon total cross section measurements compared to theoretical predictions.

I.3 Search for Parity Violation in Deuteron Photodisintegration Near Threshold.

The physics in such a measurement is basically the same as in hadron-hadron scattering. The polarized photon is used to probe the helicity of the nucleon or quark which is involved in the proton-neutron interaction.

The experiment /3/ was performed at the Chalk River linear accelerator at 3.2 and 4.0 MeV, using a polarized GaAs electron source (Fig.8). The longitudinal electron polarization is almost completely transferred to the photon beam at the end point energy. The photon beam is dumped into a D_2O container which is surrounded by neutron detectors. Theoretical calculations predict the polarized asymmetry to be smaller than 0.6×10^{-7} /13/.
The experiment is in fact the inverse of the famous Lobashev experiment $p(n,\vec{\gamma})d$ /14/, which measured the circular polarization of the emitted photon in neutron capture by protons. The photon polarization was found to be $P_\gamma <$ 0.5×10^{-6}.
The deuteron disintegration experiment was carried out at 3.2 and 4.0 MeV photon energies. At these two energies the break-up involves quite different contributions from E1 and M1 transitions in the cross section. One may therefore expect different sensitivities to diagrams involving weak boson exchange at these energies.
The same setup was used to search for PNC effects in bremsstrahlungs production. The preliminary results for both processes are given in the following table.

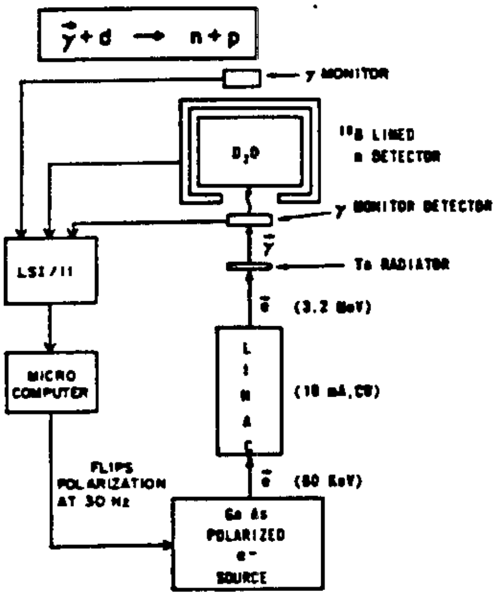

Fig. 8 Schematic setup of the Chalk River experiment to measure parity violation in photodisintegration of deuterium near threshold.

Energy	A_γ	A_n
4.0 MeV	$(.66\pm.73)\times10^{-8}$	$(2.8\pm2.8)\times10^{-8}$
3.2 MeV	$(3.0\pm1.6)\times10^{-8}$	$(7.7\pm5.3)\times10^{-8}$

At the 2σ level of accuracy this measurement yields no non-zero result. It was stated that the overall error is still dominated by systematic effects. Clearly, the measurements are not yet accurate enough to constrain the theory.

I.4 Comment on the Reported Experiments on PNC.

The experiments on PNC effects which were presented at this conference reflect achievements of intermediate energy spin physics in recent years. The high statistical accuracy and in particular the small systematic uncertainties are the result of many years of persistent efforts to understand and eliminate spurious asymmetries at the level of 10^{-8} to 10^{-6} accuracy for the various experiments. Future experiments in this field of research should be able to benefit greatly from these efforts.

II. Asymmetries in Electron Scattering From Polarized Deuterium.

II.1 Elastic Scattering From Tensorpolarized Deuterium.

The isoscalar electromagnetic current of the deuteron is specified by the three quantities G_C, G_Q, G_M, the electric charge-, electric quadrupole-, and magnetic dipole form factors. In unpolarized elastic electron deuteron scattering only G_M^2 and the combination $G_C^2 + 8/9\eta^2 G_Q^2$ ($\eta = Q^2/4M_D^2$) can be measured. A separation of G_C/G_Q requires a polarization experiment. A separate measurement of G_C and G_Q is of significant importance. In particular, G_C contains information on the short range part of the nucleon-nucleon interaction and on the relevance of mesonic exchange currents as well as of possible contributions from six quark hidden colour states in the deuteron wave function[15]. Using a tensorpolarized deuterium target, the elastic cross section writes

$$d\sigma/d\Omega = (d\sigma_o/d\Omega)[1 + F_{20}\tilde{t}_{20} + 2F_{21}\mathrm{Re}(\tilde{t}_{21}) + 2F_{22}\mathrm{Re}(\tilde{t}_{22})]$$

where the $\tilde{t}_{ij}$ are related to the target polarization, e.g., $\tilde{t}_{20} = -1/\sqrt{2}P_{zz}$, P_{zz} = alignment. The F_{ij} can be expressed in terms of the isoscalar form factors, e.g.,

$$F_{20} = -\sqrt{2}/3\eta \frac{4G_Q(G_C+(\eta/3)G_Q)+[1/2+(1+\eta)\mathrm{tg}^2(\theta/2)]G_M^2}{G_E^2+(8/9)\eta^2G_Q^2+(2/3)\eta[1+2(1+\eta)\mathrm{tg}^2(\theta/2)}\ .$$

F_{20} contains the interference term $G_C G_Q$ which makes this quantity particularly sensitive to any structure that may occur in either of the respective form factors.

Results were reported from an experiment performed at the 400 MeV VEPP-2 storage ring at Novosibirsk[16]. This experiment used a polarized deuterium gas jet target with a density of $2\mathrm{x}10^{11}$ molecules/cm^2. The instantanous luminosity was approximately 10^{29} $\mathrm{cm}^{-2}\mathrm{sec}^{-1}$. Despite this very low luminosity, the Novosibirsk group was able to measure the asymmetry F_{20} for two values of Q^2. The results are shown in Fig.9, together with data previously measured at the MIT-Bates linear accelerator[17]. Some theoretical predictions are also included. Clearly, to be sensitive to details of the deuteron wave function and to the $\gamma_v D$ coupling, data at higher values of Q^2 and with better statistics will be required.

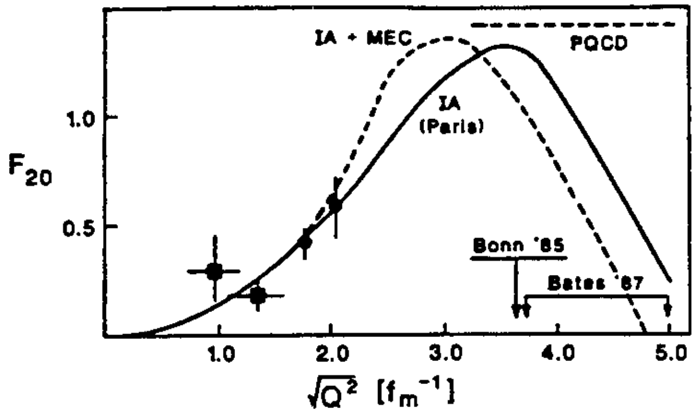

Fig. 9 Tensorpolarization asymmetry F_{20} as measured at VEPP-2 (full squares) and at MIT-Bates (full dots). Indicated are the Q^2 ranges of already performed (Bonn '85) and forthcoming (Bates '87) experiments.

It was reported that this experiment will be installed at the VEPP-3 storage ring at Novosibirsk and will continue to take data at an electron energy of 1.8 GeV. This will allow considerably higher Q^2 values to be reached.

The status of the Bonn experiment on elastic electron deuteron scattering was reported /18/. This experiment utilizes a dynamically vectorpolarized ND_3 target and obtains a sizeable tensorpolarization of $P_{zz} = 0.15$ as a byproduct. The measurement was carried out with a luminosity of $2x10^{32}$ $cm^{-2}sec^{-1}$. The scattered electrons and the recoil deuterons were detected in two magnetic spectrometers in coincidence (Fig.10), which enables a separation of scattering off free (polarized) deuterons from bound (unpolarized) deuterons in the nitrogen nucleus. The vectorpolarization does not give rise to an asymmetry in elastic scattering unless the incoming electron beam is polarized as well. Data were taken at $Q^2 = 0.5$ $(GeV/c)^2$, where the asymmetry is quite sensitive to mesonic exchange currents in the interaction. Results of this measurement should become available soon.

II.2 Inelastic Scattering From Polarized Deuterium.

The Novosibirsk group also measured the disintegration process $\vec{D}(e,pn)e'$ at $E_e = 180$ MeV, using the same apparatus as in the elastic measurement/19/. This process contains information which is quite different from elastic scattering. Unpolarized electrodisintegration of deuterium enables the extraction of the nucleon momentum distribution in the deuteron/21/. With a tensorpolarized target, the s-wave and d-wave contributions can be measured separately/16/. This provides new information on the d-wave content as well as on the importance of relativistic effects in the deuteron wave function.

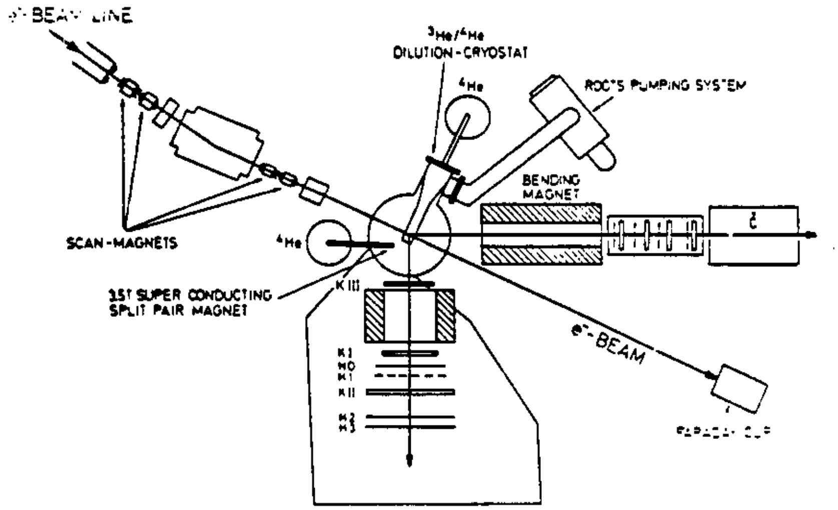

Fig. 10 Experimental set-up of the Bonn experiment to measure the elastic tensorpolarization asymmetry F_{20}. The incoming electron beam is scanned across the target front face to uniformly irradiate the polarized ND_3 target. Both scattered particles are detected in magnetic spectrometers.

Fig.11 shows the measured polarization asymmetry for a specific kinematics versus the excitation energy of the pn-system in the final state. The asymmetries appear to be large and are quite sensitive to final state interaction as well as to relativistic effects in the deuteron wave function. With the higher energy at the VEPP-3 storage ring one may expect that much higher excitation energies will be reached where a clear discrimination between relativistic and non-relativistic models should become possible.

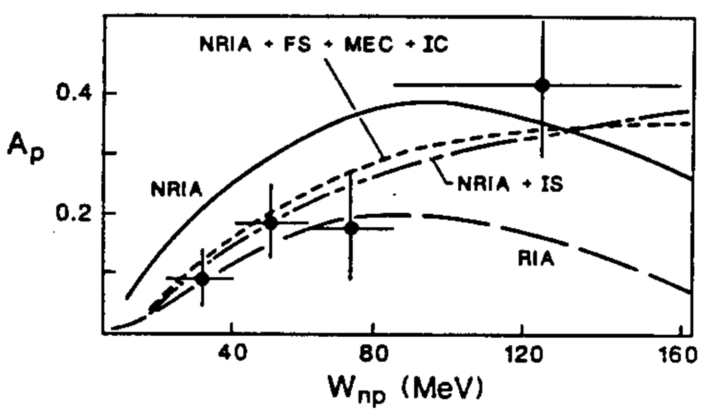

Fig. 11 Polarization asymmetry in electrodisintegration of tensor polarized deuterium. The curves labelled NRIA are non relativistic calculations including various additional contributions from final state interaction, meson exchange, and isobar currents. RIA is a calculation based on relativistic impulse approximation.

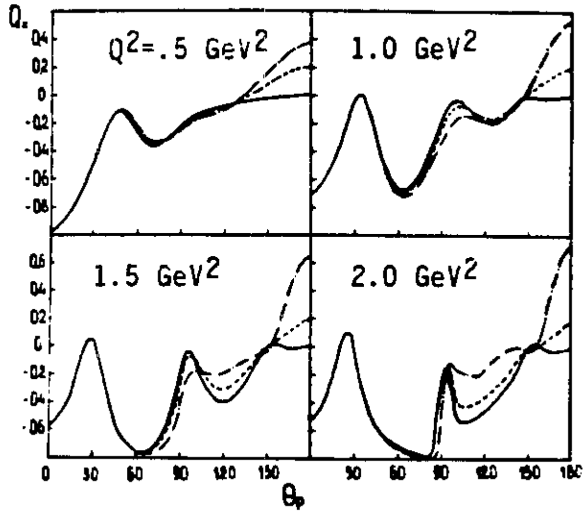

Fig. 12 Sensitivity of the polarization asymmetry Q_x to the electric formfactor of the neutron. Solid line: $G_{En}=0$; dashed line: $G_{En}=\tau G_{Mn}$; dashed-dotted line: $G_{En}=G_{Mn}/(1\text{-}5.6\tau)$. The calculation uses the Paris NN potential.

The single theoretical contribution concerned the study of polarization effects in the electrodisintegration of deuterium. Detailed calculations have been carried out to study effects of the deuteron wave function, as well as effects arising from uncertainties in our knowledge of the nucleon form factors/26/. Of particular interest here is the sensitivity of polarization asymmetries to the choice of the electric form factor of the neutron, which is poorly known experimentally. In Fig.12 the double polarization asymmetry is shown for quasielastic kinematics, using a longitudinal polarized electron beam and a polarized deuterium target with the polarization axis in the electron scattering plane perpendicular to the direction of the virtual photon. It turns out that the polarization asymmetry is quite sensitive to the choice of G_{En} if the proton is measured in backward direction or the neutron in forward direction, respectively. Measurements of this type should thus enable a model independent extraction of this fundamental quantity.

References.

1 W. Achenbach et al.; contribution to this conference.
W. Heil; presentation at this conference.
2 V. Yuan et al.; Phys. Rev. Lett. 57, 1680 (1986).
J. D. Bowman; presentation at this conference.
3 A. McDonald; presentation at this conference.
4 P. Q. Hung, J. J. Sakurai; Phys. Lett. 63B, 295 (1976).
5 C. Y. Prescott et al.; Phys. Lett. 77B, 347 (1978).
C. Y. Prescott et al.; Phys. Lett. 84B, 524 (1979).
6 P. Q. Hung, J. J. Sakurai; Annual Rev. of Nucl. a. Part. Science 31.

7 F. Dydak; CERN EP/86-121 (1986).
8 R. Balzer et al.; Phys. Rev. Lett. 44, 699 (1980).
9 R. Balzer et al.; Phys. Rev. C30, 1409 (1984).
10 N. Lockyer et al.; Phys. Rev. Lett. 45, 1821 (1980).
11 G. Nardulli, G. Preparata; Phys. Lett. 137B, 111 (1984).
12 L. S. Kisslinger, G. A. Miller; Phys. Rev. C27 (1983).
13 H. C. Lee; Phys. Rev. Lett. 41, 843 (1978).
14 V. A. Knyazkov, et al.; JETP Lett. 38, 163 (1983).
15 M. Gari, H. Hyuga; Nucl. Phys. A264, 409 (1976).
A. P. Kobushkin; Sov. J. Nucl. Phys. 28, 252 (1978).
16 D. M. Nikolenko et al.; Nucl Phys. A446, 393 (1985).
D. K. Toporkov; presentation at this conference.
17 M. E. Schulze et al.; Phys. Rev. Lett. 52, 597 (1984).
18 K. H. Althoff et al.; contribution to this conference.
W. Meyer; presentation at this conference.
19 Toporkov; presentation at this conference.
20 M. P. Rekalo, G. N. Gakh, A. P. Rekalo; contribution to this conference.
21 J. Mougey; Nucl. Phys. A358, 293 (1981).
22 J. Arvieux ; Invited talk, these proceedings.
S. L. Belostotsky; Invited talk, these proceedings.
C. Leluc; Invited talk, these proceedings.

Copies available from:

Library
CEBAF
12070 Jefferson Avenue
Newport News
Virginia 23606

The Southeastern Universities Research Association (SURA) operates the Continuous Electron Beam Accelerator Facility for the United States Department of Energy under contract DE-AC05-84ER40150.